


Many-Body Self-Interaction and Polarons

Stefano Falletta^{✉*} and Alfredo Pasquarello[✉]

Chaire de Simulation à l'Echelle Atomique (CSEA), Ecole Polytechnique Fédérale de Lausanne (EPFL), CH-1015 Lausanne, Switzerland

 (Received 10 May 2022; revised 26 August 2022; accepted 30 August 2022; published 14 September 2022)

We address the many-body self-interaction in relation to polarons in density functional theory. Our study provides (i) a unified theoretical framework encompassing many-body and one-body forms of self-interaction and (ii) an efficient semilocal scheme for charge localization. Our theoretical formulation establishes a quantitative connection between the many-body and one-body forms of self-interaction in terms of electron screening, thereby conferring superiority to the concept of many-body self-interaction. Our semilocal methodology involves the use of a weak localized potential and applies equally to electron and hole polarons. We find that polarons free from many-body self-interaction have formation energies that are robust with respect to the functional adopted.

DOI: 10.1103/PhysRevLett.129.126401

Electron self-interaction (SI) is a long-standing problem in density functional theory (DFT) [1–7] and is particularly critical in the description of polarons [8–14]. Polarons are quasiparticles involving charge localization coupled with self-induced lattice distortions. Since their prediction by Landau [15] and Pekar [16] almost a century ago, polarons have drawn a great deal of attention in physics, chemistry, and materials science [14,17–20]. The polaron stability results from the competition between the energy gain associated with the charge localization and the energy cost of the involved lattice distortions. Therefore, the polaron localization and its formation energy are sensitively affected by the description of the electron SI.

Various electronic-structure schemes have been introduced over the years to address the SI [1–13]. Most of these schemes focus on removing the one-body SI, which arises from the interaction of the excess charge with itself [1,8,9,12,13]. More recently, on the basis of a property of the exact density functional, the concept of many-body SI has been defined [2–7,10,11] as the deviation from the piecewise linearity of the total energy upon electron occupation [21]. At present, it remains unclear which of these two descriptions of the SI needs to be addressed in polaron physics.

While SI correction schemes may achieve polaron localization, the resulting energetics differs dramatically when addressing the many-body or the one-body SI. To illustrate this difference, we consider the polaron stability as obtained with the hybrid functional PBE0(α) [22], which includes a fraction α of Fock exchange. For a specific $\alpha = \alpha_k$, the functional is piecewise linear upon electron occupation and the many-body SI vanishes [10,11,23]. At variance, setting $\alpha = 1$ removes the one-body SI like in Hartree-Fock theory, apart from weaker correlation terms. In the latter case, the polaron formation energy can deviate

by several electronvolts from the result achieved with PBE0(α_k), as illustrated in Fig. 1(a) for the hole polaron in MgO. However, it should be remarked that the cancellation of the many-body SI further guarantees an accurate description of the band gap [23], which in turn gives defect energy levels in good agreement with experiment and state-of-the-art *GW* many-body calculations [24]. This strongly suggests that one should correct for the many-body rather than for the one-body SI.

In this context, it is of interest to investigate whether the notion of many-body SI could enable the accurate modeling of polarons at the semilocal level of theory. Indeed, such a semilocal scheme would bypass computationally expensive structural relaxations at the hybrid-functional level, which is particularly critical when using plane-wave basis sets. This would allow for the widespread study of

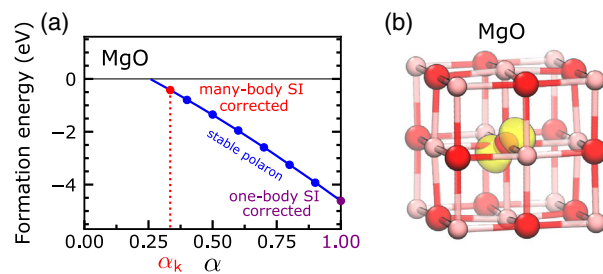


FIG. 1. (a) Formation energy as obtained with the hybrid functional PBE0(α) for the hole polaron in MgO. Negative formation energies indicate polaron stability. The many-body and the one-body self-interaction are suppressed at $\alpha = \alpha_k$ and at $\alpha = 1$, respectively. (b) Isodensity surface of the hole polaron at 5% of its maximum (Mg in pink, O in red). The hole polaron is centered on an O atom, leading to longer bonds with neighboring Mg atoms.

polarons in large systems, in high-throughput searches involving extensive databases of materials, or in molecular dynamics evolving over long time periods.

In this Letter, we first elaborate a unified theoretical framework that includes the concepts of many-body and one-body self-interaction within the same formulation. In this way, we find an analytical connection between the two forms of self-interaction in terms of the electron screening. The many-body self-interaction is shown to reduce to the one-body self-interaction in the absence of electron screening. This analysis demonstrates the preeminence of the many-body self-interaction over the one-body self-interaction. Next, we develop a semilocal scheme for removing the many-body self-interaction of polarons in density functional theory. Our approach leads to localization of both electron and hole polarons through the addition of a weak local potential to the Kohn-Sham Hamiltonian. The calculated polaron formation energies are in close agreement with the results obtained in this Letter from a hybrid functional with vanishing many-body self-interaction. This indicates that addressing the many-body self-interaction leads to robust polaron formation energies with respect to the functional adopted. As case studies, we take the electron polaron in BiVO₄ [25], the hole polaron in MgO [26,27], and the hole trapped at the Al impurity in α -SiO₂ [8,26,28–30].

We are interested in deepening the concept of many-body SI and in clarifying its relationship with one-body SI. For this purpose, we focus on the class of hybrid

functionals PBE0(α), which can cover either form of SI depending on α [Fig. 1(a)]. We denote $E^\alpha(q)$ and $\epsilon_p^\alpha(q)$ the total energy and the polaron level corresponding to a fractional polaron charge q . The targeted piecewise linear behavior is achieved at $\alpha = \alpha_k$ and is such that $dE^{\alpha_k}(q)/dq = -\epsilon_p^{\alpha_k}$ [31]. Hence, we express the many-body SI correction to the PBE0(α) energy as

$$\Delta E^\alpha(q) = \underbrace{(E^\alpha(0) - q\epsilon_p^{\alpha_k})}_{\text{linear}} - \underbrace{E^\alpha(q)}_{\text{convex or concave}}, \quad (1)$$

which represents the deviation from the piecewise linearity of the PBE0(α) total energy as a function of the fractional charge.

Here, we focus on correcting the functional with $\alpha = 0$ corresponding to the semilocal Perdew-Burke-Ernzerhof (PBE) level of theory [32]. The many-body-SI corrections can be generalized to a generic PBE0(α) hybrid functional [33]. The energy $E^0 + \Delta E^0|_{\text{mb}}$ is piecewise linear as a function of q , as illustrated in Fig. 2(a) for the hole polaron in MgO. The respective polaron level is constant and assumes the value $\epsilon_p^{\alpha_k}$ [Fig. 2(b)]. We re-elaborate Eq. (1) by taking the polaron level $\epsilon_p^\alpha(q)$ to depend linearly on both α [11,23,34–38] and q [6,39]. This allows us to define a fractional charge q_k such that $\epsilon_p^{\alpha_k} = \epsilon_p^\alpha(q_k)$, irrespective of α [33]. In particular, $\epsilon_p^{\alpha_k} = \epsilon_p^0(q_k)$ [Fig. 2(b)]. Moreover, through Janak's theorem [31], the total energy $E^0(q)$ is thus quadratic in q , leading to [33]

$$\Delta E^0(q)|_{\text{mb}} = -[(q - q_k)^2 - q_k^2] \left\{ E_H \left[\frac{dn}{dq} \right] + \frac{1}{2} \sum_{\sigma\sigma'} \int d\mathbf{r}d\mathbf{r}' \frac{\delta^2 E_{\text{xc}}[n_\uparrow, n_\downarrow]}{\delta n_\sigma(\mathbf{r}) \delta n_{\sigma'}(\mathbf{r}')} \frac{dn_\sigma(\mathbf{r})}{dq} \frac{dn_{\sigma'}(\mathbf{r}')}{dq} \right\}, \quad (2)$$

where E_H is the Hartree energy, E_{xc} the exchange-correlation energy, n_σ the total density in the spin channel σ , and $n = n_\uparrow + n_\downarrow$. In Eq. (2), the electron screening is accounted for through the derivatives $dn_\sigma(q)/dq$, which represent the response of the electronic structure to the variation of the polaron charge (Fig. 3).

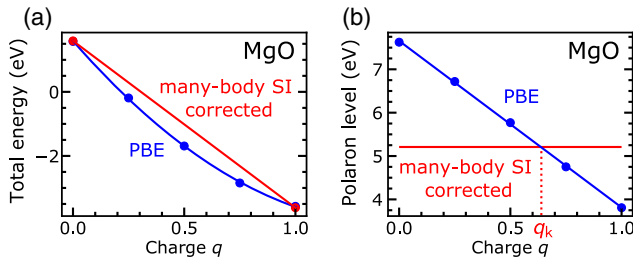


FIG. 2. Many-body self-interaction corrected (a) total energy and (b) polaron level as a function of the charge q , in comparison with the PBE values, obtained for the geometry and wave functions of a localized hole polaron in MgO.

To establish a connection between the many-body and one-body forms of SI, we remark that the one-body SI corrections to $E^0(q)$ can be defined from energy differences between the cases $\alpha = 1$ (Hartree-Fock-like) and $\alpha = 0$ (PBE). Using the generalization of Eq. (2) to the PBE0(α) functional, we find [33]

$$\Delta E^0(q)|_{\text{ob}} = \frac{1}{\alpha_k} \Delta E^0(q)|_{\text{mb}}, \quad (3)$$

which reveals that the many-body SI and the one-body SI are related to each other through α_k . This hints at a deep connection with the electron screening, as represented by the high-frequency dielectric constant ϵ_∞ . Since the asymptotic potential of the exact functional is given by $-1/(\epsilon_\infty r)$ [7,40], one infers $\alpha_k \simeq 1/\epsilon_\infty$ [41,42]. This is further supported by the accurate band gaps achieved with the functional PBE0($1/\epsilon_\infty$) for a large variety of materials [23,43,44] upon proper consideration of effects due to thermal vibrations, spin-orbit coupling, electron-hole

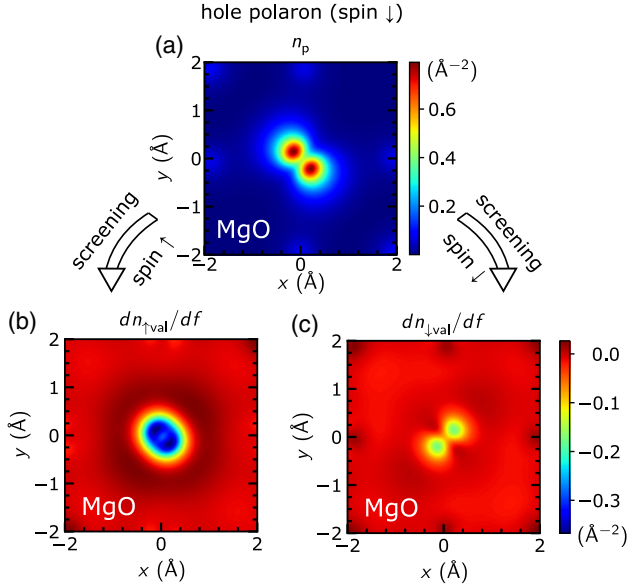


FIG. 3. (a) Polaron density n_p and (b) and (c) variation of the valence-electron densities $n_{\uparrow\text{val}}$ and $n_{\downarrow\text{val}}$ upon occupation f of the hole polaron state in MgO. The densities are integrated over the z direction and plotted in the xy plane. For hole polarons in the spin channel \downarrow , $n_{\uparrow} = n_{\uparrow\text{val}}$ and $n_{\downarrow} = n_{\downarrow\text{val}} - n_p$.

interaction, and magnetic ordering [45–47]. Hence, $\Delta E^0|_{\text{mb}} \simeq \Delta E^0|_{\text{ob}}/\epsilon_{\infty}$, which quantifies the relative magnitude of these SI energies. Moreover this relation carries similarity with the necessity of including the dielectric constant in the Coulomb kernel when correcting the exciton binding energy in Hartree-Fock theory [48,49]. This supports the deeper physical significance of the many-body SI with respect to the one-body SI. The role of the screening in the SI can be further highlighted when turning off the response of the valence electrons to the polaron charge. Indeed, when neglecting the variation of the valence wave functions with q and the weaker correlation terms, one finds that the piecewise linearity is satisfied for $\alpha_k^{\text{bare}} = 1$ [33]. In the absence of electron screening, the many-body SI thus coincides with the one-body SI [Eq. (3)]. This analysis clarifies the relationship between the two forms of SI in terms of the electron screening conferring superiority to the notion of many-body SI. Comparisons with previous forms of SI [5,12,13] can be found in Ref. [33].

Next, we aim to address the many-body SI at the semilocal level of theory through self-consistent calculations. However, the variational minimization of the functional $E^0 + \Delta E^0|_{\text{mb}}$ carries limitations. First, it would require the knowledge of the parameter q_k , which is inherently related to the hybrid functional formulation. Second, polaron localization would not be guaranteed because the SI of the valence band states would remain uncorrected. This results in a competition between localized and delocalized states, which can prevent polaron localization. To overcome these limitations, we assume that

polaron stabilization can be achieved through the addition of a weak local potential in the Kohn-Sham Hamiltonian. This directly targets the energy separation between the localized and the delocalized states, which are generally in close energetic competition [50,51]. For each spin channel σ , we denote this potential as V_{σ}^{γ} , where γ regulates its strength. This leads to the Kohn-Sham equations

$$(\mathcal{H}_{\sigma}^0 + V_{\sigma}^{\gamma})\psi_{i\sigma}^{\gamma} = \epsilon_{i\sigma}^{\gamma}\psi_{i\sigma}^{\gamma}, \quad (4)$$

where \mathcal{H}_{σ}^0 is the semilocal PBE Hamiltonian [32], and $\psi_{i\sigma}^{\gamma}$ and $\epsilon_{i\sigma}^{\gamma}$ are the resulting wave functions and energy levels, respectively. We denote Q the integer polaron charge. Hence, for electron polarons $Q = -1$, while for hole polarons $Q = +1$. Self-consistent electronic and structural relaxations lead to the polaron geometry \mathbf{R}_Q^{γ} and to the polaron energy level ϵ_p^{γ} corresponding to the highest-occupied (lowest unoccupied) state in the case of electron (hole) polaron.

We find that an expression of V_{σ}^{γ} favoring polaron localization is given by

$$V_{\sigma}^{\gamma}(q) = q\gamma \frac{\partial V_{\text{xc}\sigma}(q)}{\partial q}, \quad (5)$$

where $V_{\text{xc}\sigma}$ is the exchange-correlation potential in the spin channel σ . In Eq. (5), we introduce a dependence on the fractional polaron charge q such that one recovers the PBE functional for $q = 0$. The potential V_{σ}^{γ} features several convenient aspects. In particular, the electronic structure and the structural relaxations can be achieved through the use of standard algorithms and the computational overhead with respect to PBE calculations is negligible [33]. The localization of electron and hole polarons is achieved in an equivalent way, since the same potential V_{σ}^{γ} applies to all states.

To correct the many-body SI of the polaron, we determine a suitable value for γ , denoted γ_k . Through Janak's theorem [31], this is achieved by imposing the condition of constant energy level upon varying polaron occupation,

$$\left. \frac{d}{dq} \epsilon_p^{\gamma}(q) \right|_{\gamma=\gamma_k} = 0. \quad (6)$$

In the search for γ_k , γ and \mathbf{R}_Q^{γ} are varied self-consistently until the condition in Eq. (6) is satisfied. The polaron formation energy is defined as [52,53]

$$E_f^{\gamma}(Q) = E^{\gamma}(Q) - E_{\text{ref}}^{\gamma}(0) + Q\epsilon_b^{\gamma}, \quad (7)$$

where $E^{\gamma}(Q)$ and $E_{\text{ref}}^{\gamma}(0)$ are the total energies of the polaron and of the pristine system, respectively, and ϵ_b^{γ} is the band edge corresponding to the delocalized state. For $\gamma = \gamma_k$, the total energy at fixed $\mathbf{R}_Q^{\gamma_k}$ is piecewise linear upon polaron occupation:

$$E^{\gamma k}(Q) = E^{\gamma k}(0) - Q\epsilon_p^{\gamma k}. \quad (8)$$

Thus, the polaron formation energy at $\gamma = \gamma_k$ is given by

$$E_f^{\gamma k}(Q) = Q(\epsilon_b^{\gamma k} - \epsilon_p^{\gamma k}) + [E^{\gamma k}(0) - E_{\text{ref}}^{\gamma k}(0)]. \quad (9)$$

The first and the second term on the right-hand side of Eq. (9) correspond to the gain from electron localization and to the cost from lattice distortions, respectively. We remark that $\epsilon_b^{\gamma k}$, $E^{\gamma k}(0)$, and $E_{\text{ref}}^{\gamma k}(0)$ coincide with their respective PBE quantities because of the vanishing prefactor q in the potential of Eq. (5).

We apply our semilocal scheme to the three case systems. The electronic-structure is obtained within a plane-wave density functional approach, in which core-valence interactions are described by pseudopotentials [54], as implemented in the QUANTUM ESPRESSO suite [55]. We use 96-atom, 64-atom, and 72-atom supercells for BiVO₄, MgO, and α -SiO₂, respectively. The lattice parameters are optimized at the PBE level [32] for the pristine systems. We sample the Brillouin zone at the Γ point and set the energy cutoff to 100 Ry in all cases. All total energies and polaron levels are corrected for finite-size effects through a scheme that properly accounts for ionic polarizations [27]. To simplify the notation, these corrections are implicitly assumed throughout our Letter. The calculations yield localized polarons for γ above a threshold value in all cases. We find γ_k by performing structural relaxations for several values of γ until Eq. (6) is satisfied. This gives $\gamma_k = 1.80, 1.96,$ and 2.40 for BiVO₄, MgO, and α -SiO₂, respectively. As illustrated in Fig. 4(a) for the hole polaron in MgO, the potential $V_{\sigma_p}^{\gamma k}$ opposes the effect of the electrostatic potential V_{elec} generated by the polaron, thus favoring polaron localization. This potential $V_{\sigma_p}^{\gamma k}$ is indeed weak compared to V_{elec} . The resulting bond lengths and formation energies are given in Table I.

It is of interest to investigate the robustness of the polaron properties upon correcting the many-body SI within different electronic-structure schemes. For this purpose, we consider polarons free from many-body SI

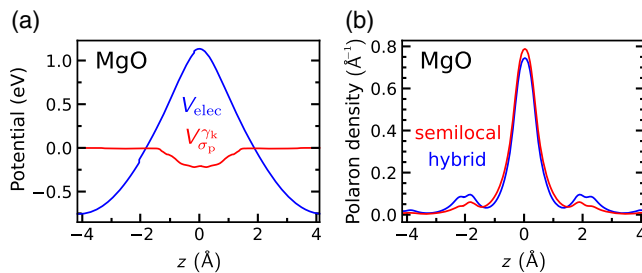


FIG. 4. (a) The potential $V_{\sigma_p}^{\gamma k}(Q)$ and the electrostatic potential V_{elec} generated by the polaron charge, averaged over xy planes, for the hole polaron in MgO. (b) Polaron densities integrated over xy planes obtained with schemes free from many-body self-interaction.

as obtained with the hybrid functional PBE0(α_k). Similarly to Eq. (6), α_k then satisfies the following condition [21,23]:

$$\left. \frac{d}{dq} \epsilon_p^{\alpha}(q) \right|_{\alpha=\alpha_k} = 0. \quad (10)$$

In the search for α_k , α and the corresponding polaron geometry \mathbf{R}_Q^{α} are varied self-consistently until Eq. (10) is satisfied. Analogously to Eq. (9), the polaron formation energy at $\alpha = \alpha_k$ is expressed as

$$E_f^{\alpha k}(Q) = Q(\epsilon_b^{\alpha k} - \epsilon_p^{\alpha k}) + [E^{\alpha k}(0) - E_{\text{ref}}^{\alpha k}(0)]. \quad (11)$$

We find $\alpha_k = 0.14, 0.34,$ and 0.45 for BiVO₄, MgO, and α -SiO₂, respectively. The corresponding formation energies are reported in Table I.

The polaron densities obtained with the semilocal and hybrid functional schemes are very similar [Fig. 4(b)]. Accordingly, a close correspondence is also found for the polaron structures (Table I). All bond lengths differ by less than 0.03 Å, with the exception of the weak Al-O bond in α -SiO₂ differing by 0.12 Å. The variations in formation energies amount to 0.19, 0.03, and 0.36 eV for BiVO₄, MgO, and α -SiO₂ (Table I), corresponding to 5.6%, 0.4%, and 3.4% of their respective band gaps. This quantitative agreement is highly satisfactory in consideration of the large variations of E_f^{α} with α found in Fig. 1(a). It can be shown that this result stems from the fact that the polaron state and the respective band states belong to the same electron manifold [33]. This analysis supports that addressing the many-body SI confers robustness to the polaron properties irrespective of the functional adopted.

In conclusion, our Letter addresses the many-body self-interaction in relation to polarons in density functional theory. First, we derive a unified formulation for the many-body and one-body self-interaction, thereby revealing an analytical connection between the two forms of self-interaction in terms of the electron screening. This analysis confers conceptual superiority to the many-body self-interaction over the one-body self-interaction. Second, taking advantage of the notion of many-body self-interaction, we develop a scheme for achieving localized polarons at the semilocal level of theory. Moreover, we

TABLE I. Relevant bond lengths (V-O, Mg-O, short/long Al-O) and polaron formation energies obtained with semilocal and hybrid functional schemes free from many-body self-interaction. Bond lengths in Å, energies in eV.

	Bond lengths		Formation energy	
	Semilocal	Hybrid	Semilocal	Hybrid
BiVO ₄	1.82	1.80	-0.44	-0.63
MgO	2.23	2.20	-0.50	-0.53
α -SiO ₂	1.71/2.03	1.69/1.91	-2.75	-3.11

find that polarons free from many-body self-interaction have formation energies that are robust with respect to the functional adopted. Hence, the present study leads to significant developments to the long-standing problem of self-interaction, from both the conceptual and the methodological point of view.

The present semilocal scheme is available for incorporation into the next official release of the QUANTUM ESPRESSO suite [55].

This work has been realized in relation to the National Center of Competence in Research (NCCR) ‘‘Materials’ Revolution: Computational Design and Discovery of Novel Materials (MARVEL)’’ of the SNSF (Grant No. 182892). The calculations have been performed at the Swiss National Supercomputing Centre (CSCS) (grant under projects ID s1122 and mr25). Material associated with this paper can be found on Materials Cloud [56].

*stefano.falletta@epfl.ch

- [1] J. P. Perdew and A. Zunger, *Phys. Rev. B* **23**, 5048 (1981).
- [2] P. Mori-Sánchez, A. J. Cohen, and W. Yang, *J. Chem. Phys.* **125**, 201102 (2006).
- [3] A. J. Cohen, P. Mori-Sánchez, and W. Yang, *Science* **321**, 792 (2008).
- [4] T. Schmidt and S. Kümmel, *Phys. Rev. B* **93**, 165120 (2016).
- [5] S. Lany and A. Zunger, *Phys. Rev. B* **80**, 085202 (2009).
- [6] V. Atalla, I. Y. Zhang, O. T. Hofmann, X. Ren, P. Rinke, and M. Scheffler, *Phys. Rev. B* **94**, 035140 (2016).
- [7] L. Kronik and S. Kümmel, *Phys. Chem. Chem. Phys.* **22**, 16467 (2020).
- [8] M. d’Avezac, M. Calandra, and F. Mauri, *Phys. Rev. B* **71**, 205210 (2005).
- [9] J. VandeVondele and M. Sprik, *Phys. Chem. Chem. Phys.* **7**, 1363 (2005).
- [10] B. Sadigh, P. Erhart, and D. Åberg, *Phys. Rev. B* **92**, 075202 (2015).
- [11] S. Kokott, S. V. Levchenko, P. Rinke, and M. Scheffler, *New J. Phys.* **20**, 033023 (2018).
- [12] W. H. Sio, C. Verdi, S. Poncé, and F. Giustino, *Phys. Rev. Lett.* **122**, 246403 (2019).
- [13] W. H. Sio, C. Verdi, S. Poncé, and F. Giustino, *Phys. Rev. B* **99**, 235139 (2019).
- [14] C. Franchini, M. Reticcioli, M. Setvin, and U. Diebold, *Nat. Rev. Mater.* **6**, 560 (2021).
- [15] L. Landau, *Phys. Z. Sowjetunion* **3**, 664 (1933).
- [16] S. Pekar, *Zh. Eksp. Teor. Fiz.* **16**, 341 (1946).
- [17] H. Fröhlich, H. Pelzer, and S. Zienau, *Lond. Edinb. Dubl. Philos. Mag. J. Sci.* **41**, 221 (1950).
- [18] T. Holstein, *Ann. Phys. (N.Y.)* **8**, 325 (1959).
- [19] J. T. Devreese and A. S. Alexandrov, *Rep. Prog. Phys.* **72**, 066501 (2009).
- [20] J. L. Bredas and G. B. Street, *Acc. Chem. Res.* **18**, 309 (1985).
- [21] J. P. Perdew, R. G. Parr, M. Levy, and J. L. Balduz, *Phys. Rev. Lett.* **49**, 1691 (1982).
- [22] J. P. Perdew, M. Ernzerhof, and K. Burke, *J. Chem. Phys.* **105**, 9982 (1996).
- [23] G. Miceli, W. Chen, I. Reshetnyak, and A. Pasquarello, *Phys. Rev. B* **97**, 121112 (2018).
- [24] W. Chen and A. Pasquarello, *Phys. Rev. B* **96**, 020101(R) (2017).
- [25] J. Wiktor, F. Ambrosio, and A. Pasquarello, *ACS Energy Lett.* **3**, 1693 (2018).
- [26] J. B. Varley, A. Janotti, C. Franchini, and C. G. Van de Walle, *Phys. Rev. B* **85**, 081109 (2012).
- [27] S. Falletta, J. Wiktor, and A. Pasquarello, *Phys. Rev. B* **102**, 041115(R) (2020).
- [28] G. Pacchioni, F. Frigoli, D. Ricci, and J. A. Weil, *Phys. Rev. B* **63**, 054102 (2000).
- [29] J. Lægsgaard and K. Stokbro, *Phys. Rev. Lett.* **86**, 2834 (2001).
- [30] M. Gerosa, C. Di Valentin, C. E. Bottani, G. Onida, and G. Pacchioni, *J. Chem. Phys.* **143**, 111103 (2015).
- [31] J. F. Janak, *Phys. Rev. B* **18**, 7165 (1978).
- [32] J. P. Perdew, K. Burke, and M. Ernzerhof, *Phys. Rev. Lett.* **77**, 3865 (1996).
- [33] S. Falletta and A. Pasquarello, companion paper, *Phys. Rev. B* **106**, 125119 (2022).
- [34] N. Österbacka, P. Erhart, S. Falletta, A. Pasquarello, and J. Wiktor, *Chem. Mater.* **32**, 8393 (2020).
- [35] T. Bischoff, J. Wiktor, W. Chen, and A. Pasquarello, *Phys. Rev. Mater.* **3**, 123802 (2019).
- [36] T. Bischoff, I. Reshetnyak, and A. Pasquarello, *Phys. Rev. B* **99**, 201114(R) (2019).
- [37] P. Deák, Q. Duy Ho, F. Seemann, B. Aradi, M. Lorke, and T. Frauenheim, *Phys. Rev. B* **95**, 075208 (2017).
- [38] J. Yang, S. Falletta, and A. Pasquarello, *J. Phys. Chem. Lett.* **13**, 3066 (2022).
- [39] S. Yang, A. T. Brant, and L. E. Halliburton, *Phys. Rev. B* **82**, 035209 (2010).
- [40] S. Refaely-Abramson, M. Jain, S. Sharifzadeh, J. B. Neaton, and L. Kronik, *Phys. Rev. B* **92**, 081204(R) (2015).
- [41] A. Alkauskas, P. Broqvist, and A. Pasquarello, *Phys. Status Solidi B* **248**, 775 (2011).
- [42] M. A. L. Marques, J. Vidal, M. J. T. Oliveira, L. Reining, and S. Botti, *Phys. Rev. B* **83**, 035119 (2011).
- [43] J. H. Skone, M. Govoni, and G. Galli, *Phys. Rev. B* **89**, 195112 (2014).
- [44] W. Chen, G. Miceli, G.-M. Rignanese, and A. Pasquarello, *Phys. Rev. Mater.* **2**, 073803 (2018).
- [45] J. Wiktor, I. Reshetnyak, F. Ambrosio, and A. Pasquarello, *Phys. Rev. Mater.* **1**, 022401(R) (2017).
- [46] J. Wiktor, I. Reshetnyak, M. Strach, M. Scarongella, R. Buonsanti, and A. Pasquarello, *J. Phys. Chem. Lett.* **9**, 5698 (2018).
- [47] G. Capano, F. Ambrosio, S. Kampouri, K. C. Stylianou, A. Pasquarello, and B. Smit, *J. Phys. Chem. C* **124**, 4065 (2020).
- [48] F. Bassani, G. P. Parravicini, R. A. Ballinger, and J. L. Birman, *Phys. Today* **29**, No. 3, 58 (1976).
- [49] T. M. Henderson, J. Paier, and G. E. Scuseria, *Phys. Status Solidi (b)* **248**, 767 (2011).
- [50] J. L. Gavartin, P. V. Sushko, and A. L. Shluger, *Phys. Rev. B* **67**, 035108 (2003).

- [51] A. Carvalho, A. Alkauskas, A. Pasquarello, A. K. Tagantsev, and N. Setter, *Phys. Rev. B* **80**, 195205 (2009).
- [52] C. Freysoldt, B. Grabowski, T. Hickel, J. Neugebauer, G. Kresse, A. Janotti, and C. G. Van de Walle, *Rev. Mod. Phys.* **86**, 253 (2014).
- [53] H.-P. Komsa, T. T. Rantala, and A. Pasquarello, *Phys. Rev. B* **86**, 045112 (2012).
- [54] M. van Setten, M. Giantomassi, E. Bousquet, M. Verstraete, D. Hamann, X. Gonze, and G.-M. Rignanese, *Comput. Phys. Commun.* **226**, 39 (2018).
- [55] P. Giannozzi *et al.*, *J. Phys. Condens. Matter* **21**, 395502 (2009).
- [56] S. Falletta and A. Pasquarello (2022), [10.24435/material-scloud:7p-gy](https://arxiv.org/abs/10.24435/material-scloud:7p-gy).